Timing of Gas Generation in the Cretaceous Milk River Formation, Southeastern Alberta and Southwestern Saskatchewan – Evidence from Authigenic Carbonates

Neil S. Fishman [1], Jennie L. Ridgley [1], and Donald L. Hall [2]

Fishman, N.S., Ridgley, J.L., Hall, D.L. (2001): Timing of gas generation in the Cretaceous Milk River Formation, southeastern Alberta and southwestern Saskatchewan – evidence from authigenic carbonates; *in* Summary of Investigations 2001, Volume 1, Saskatchewan Geological Survey, Sask. Energy Mines, Misc. Rep. 2001-4.1.

1. Introduction

The marine Cretaceous Milk River Formation in southeastern Alberta and southwestern Saskatchewan (Figure 1) contains abundant natural gas and contributes significantly to the >4.2 x 10^{11} m^3 (>15 trillion cubic feet) of estimated shallow gas resources in the region (Energy Resources Conservation Board, 1977). The formation is both source and reservoir rock (Ridgley *et al.*, 1999), and the contained gas is defined as a continuous-type accumulation for the purposes of exploration and resource assessments (Attanazi and Schmoker, 1997; Ridgley *et al.*, 1999). Although the unit has been previously studied, uncertainties remain concerning the timing of gas generation. During the present study, we found that the key to understanding when gas generation occurred is the recognition that the gas is biogenic. Carbon isotopic values (Figure 2) for methane in Milk River Formation-produced gas range from -66 to -75 ‰ (Fuex, 1977; Rice and Claypool, 1981; Hankel *et al.*, 1989; P. Lillis, U.S. Geological Survey, pers. comm., 2000), which is typical for primary biogenic gas generated early in the post-depositional history of marine sediments (Rice and Claypool, 1981; Whiticar *et al.*, 1986). Compositionally, the gas is dry, containing >99.45% methane (Fuex, 1977; Rice and Claypool, 1981; P. Lillis, U.S. Geological Survey, pers. comm., 2000), which is also typical of biogenic gas (Bernard *et al.*, 1976; Weber and Maximov, 1976; Rice and Claypool, 1981; Gautier, 1985).

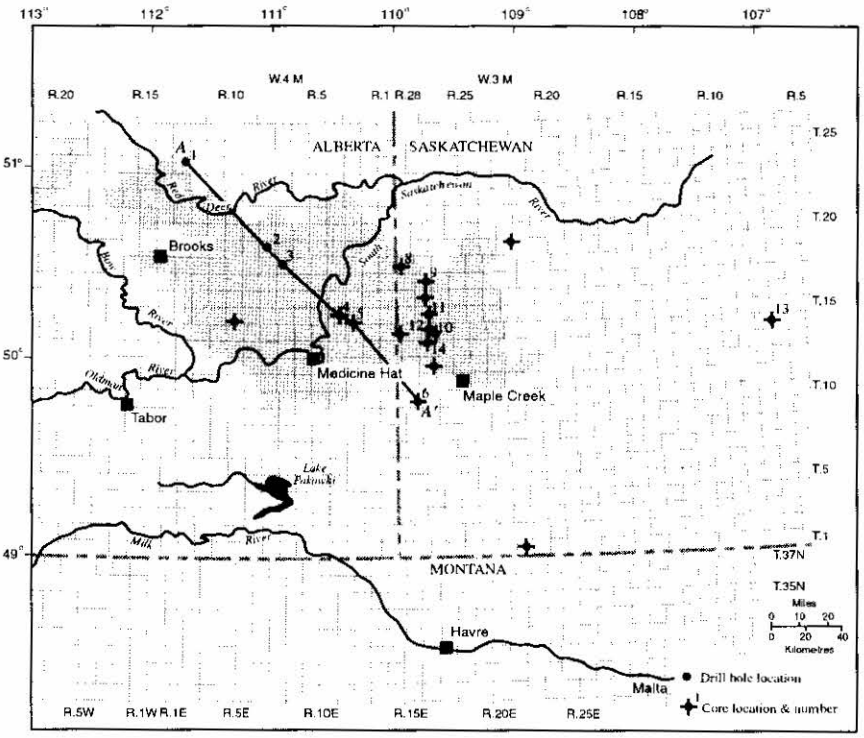

Figure 1 - Map showing locations of the study area and sampled cores. A-A' is the line of cross section in Figure 5. Grey areas indicate southeast Alberta gas fields.

The timing of gas generation in the Milk River Formation is uncertain in part because methanogenesis can occur whenever conditions in the rocks permit anaerobic bacteria, which are responsible for gas generation, to thrive (Rice and Claypool, 1981). Conditions favourable for bacterial methanogenesis include: (1) an anoxic environment; (2) appropriate temperatures (optimally 40° to 60°C, but any temperatures from 0° to 75°C are tolerable); (3) presence of organic matter; (4) low sulphate content of pore waters; and (5) sufficient permeability to allow for continuous water flow and adequate pore space for the bacteria to exist. That methanogenesis could have occurred at various times in the post-depositional history of the Milk River Formation is plausible insofar as the unit has not experienced burial

[1] U.S. Geological Survey, Central Region, Energy Resources Team, MS939, P.O. Box 25046, DFC, Denver, CO 80225-0046.
[2] Fluid Inclusion Technologies, Inc., 2217 North Yellowood Avenue, Broken Arrow, OK 74012-9106.

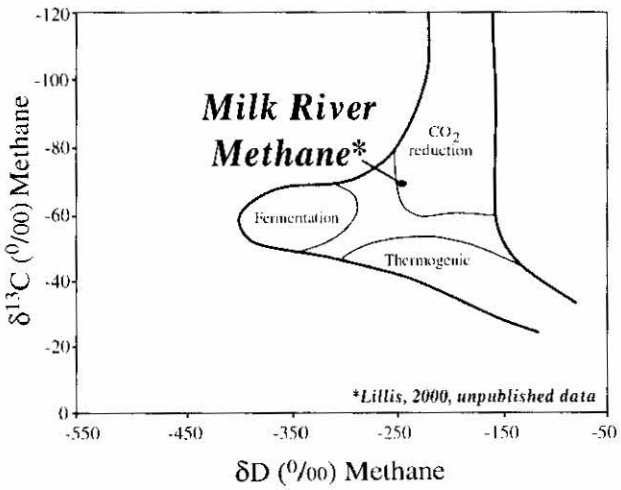

Figure 2 - Diagram on which is plotted the carbon and deuterium isotopes of natural gas, generated by different processes (modified from Whiticar et al., 1986). Analyzed samples from the Milk River Formation plot in the area of CO_2 reduction, typical of gas generated in biogenic systems.

temperatures exceeding that lethal to methanogenic bacteria. Burial reconstruction studies (Corbet and Bethke, 1992) indicate that temperatures in the unit never exceeded about 45°C (Figure 3). The shallow burial history of the Milk River Formation is consistent with the fact that Cretaceous units stratigraphically below it are thermally immature (Creaney *et al.*, 1994). Formation temperatures throughout the burial history of the Milk River Formation do not, therefore, preclude the possibility of methanogenesis having occurred at various times. However, at about 65 Ma, the Milk River Formation was buried to a maximum depth of about 1.3 km (Corbet and Bethke, 1992), slightly greater than the one kilometre depth below which primary microbial methanogenesis is generally observed to have ceased (Rice and Claypool, 1981).

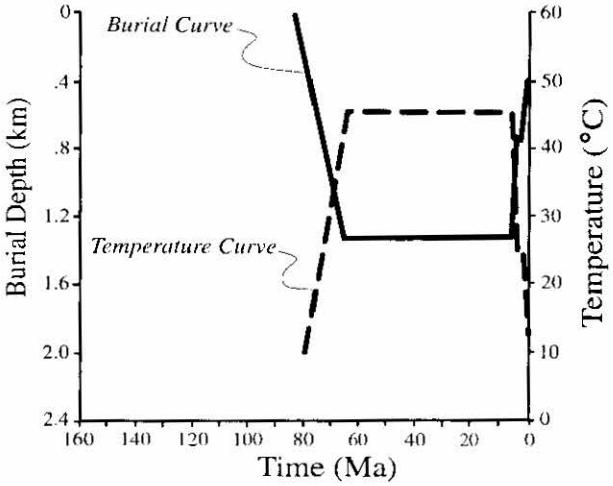

Figure 3 - Burial curve for the Milk River Formation (approximately along Township 1 in southern Alberta, after Corbet and Bethke, 1992). The Milk River Formation was buried no deeper than about 1.3 km, so maximum formation temperature was about 45°C.

Consequently, whether significant methane generation occurred when the formation was buried to depths greater than one kilometre is uncertain. As the unit was at depths of less than one kilometre for more than 15 m.y. prior to maximum burial, as well as during approximately the last seven m.y. when tectonic uplift affected the region (Figure 3), time was plentiful during which ideal microbial methanogenic conditions may have prevailed.

To address the question of timing of methane generation in the Milk River Formation, we conducted a petrologic study to determine the post-depositional alteration history of the unit, and constructed a temporal framework in which gas generation may be placed. In this paper, we present the results of petrographic, isotopic, and fluid inclusion analyses and draw preliminary conclusions.

2. Depositional History of the Milk River Formation

Although formally referenced as the Alderson Member of the Lea Park Formation (Figure 4), this stratigraphic unit is typically named the Milk River Formation by gas producers in the region, and we have chosen to use this in our study. The Milk River Formation is one of several siliciclastic units that were deposited during Late Cretaceous time in the Western Interior Seaway. Detailed examination of cores and wireline logs reveals seven distinct marine lithofacies in the formation (Ridgley, 2000) that correspond to different depositional environments (Figure 5). Interpretations of lithofacies indicate that they were deposited in delta front, coastal, shoreface, inner shelf, and outer shelf environments (Ridgley, 2000). Recently documented major erosional surfaces within the formation point to two previously unrecognized sea-level falls followed by marine transgressions (O'Connell *et al.*, 1999;

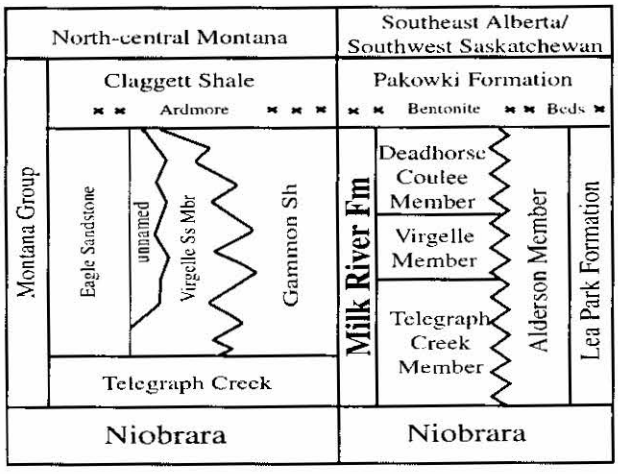

Figure 4 - Stratigraphic chart showing members of the Upper Cretaceous Milk River Formation (also referred to as the Alderson Member of the Lea Park Formation), in southern Alberta and Saskatchewan, and correlative stratigraphic units in Montana.

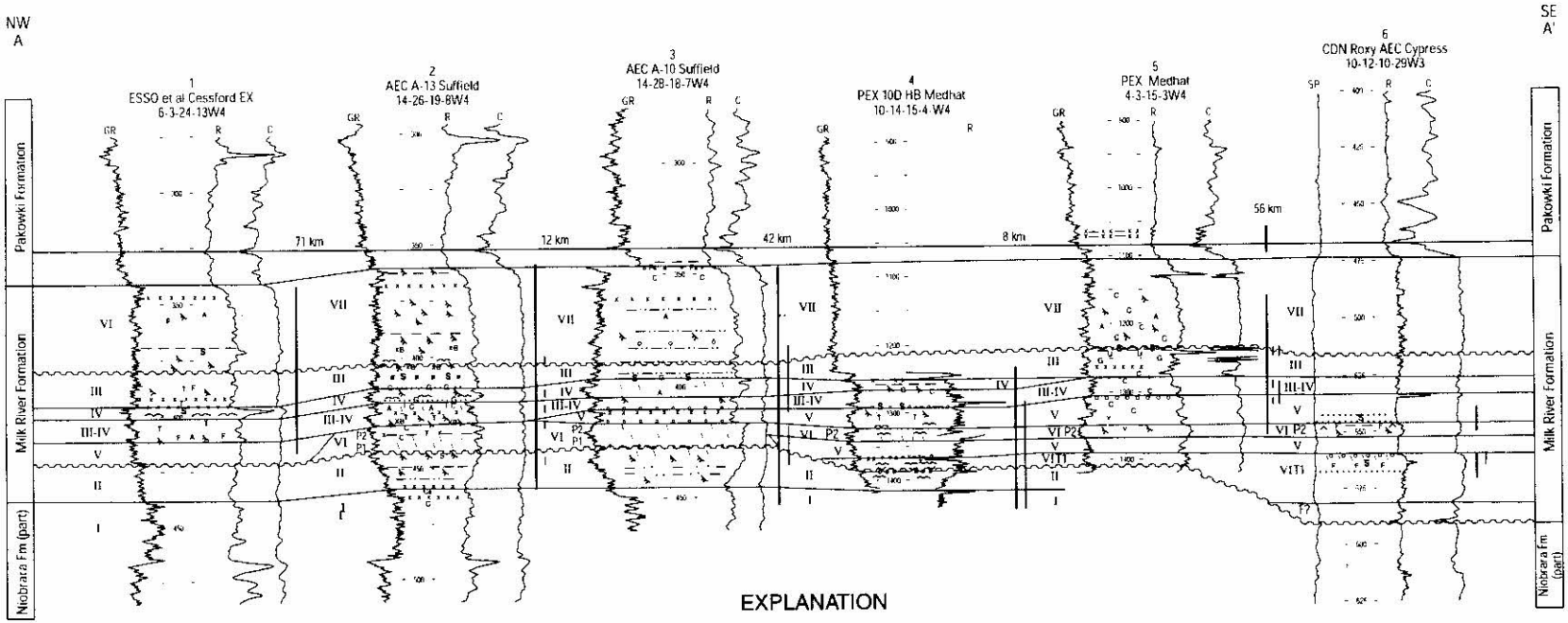

EXPLANATION

- Hummocky cross stratification
- Swaley cross stratification
- Indeterminate low angle cross stratification
- Current ripples
- F Flaser bedding
- Coarse sandstone layers
- Mudstone
- Siltstone
- Cs Coccolithic shale
- v Vuggy
- x Bentonite
- s Siderite
- Siderite clasts or conglomerate clasts
- Intraformational siderite clasts
- Fractures
- A Coiled ammonite fragments
- U *Arenicolites* burrows
- T *Terebellina* sp burrows
- Fs Fish fragments
- Chert grains or coarse grit
- xB Biotite-rich rocks
- C Carbonaceous
- G Glauconite
- Cored interval
- I Offshore facies
- II Offshore-transition facies
- III Inner to outer shelf facies
- IV Shelf sandstone facies
- V Inner shelf to outer estuarine facies
- VI Coastal sandstone facies
- VII Amalgamated shoreline sandstone and mudstone facies
- F? Fluvial facies
- Tested interval
- P 1 Regressive shoreface sand
- T 1 Transgressive shoreface sand
- Unconformity

Figure 5 - Cross section A-A' (see Figure 1 for location), showing various lithofacies that occur in the Milk River Formation, as well as simplified sedimentary structures (modified from Ridgley, 2000). Depths for wells 1 to 3 and 6 are in metres, whereas depths for wells 4 and 5 are in feet. (Gr, gamma ray; R, resistivity; C, conductivity; and SP, spontaneous potential).

Ridgley, 2000). Although attempts have been made to determine the influence of depositional facies and unconformities on gas production, the possible control these features had on gas generation and trapping is unclear.

Lithologies of the Milk River Formation include sandstone, siltstone, mudstone, and shale. Although the different lithofacies suggest variations in wave energy in the different depositional environments, the maximum grain size in all lithologies is fine sand. Grain sizes in sandstones range from fine to very fine, and sorting from moderate to poor. Modal analyses indicate that the sandstones are lithic-rich (see Table 1). Grains typically comprise, in decreasing abundance, quartz, rock fragments, dolomite, glauconitic grains, and feldspar (Table 1). Varying amounts of organic detritus are also present (Table 1). Of the detrital constituents, only some plagioclase and chert have been partially dissolved, probably mostly in early phases of the alteration history of the formation as these dissolved areas have themselves been filled with early authigenic cement.

3. Methods

Petrographic analyses of 81 thin sections from 16 different cores were used to establish paragenetic relations of authigenic phases and other textural features that bear on the alteration history of the formation. Thin sections were made after impregnation of the rock chip with blue epoxy, then were stained with sodium cobaltinitrite to assist in identifying potassium feldspar. The thin sections were also stained with a mixture of alizarin red-S and potassium ferricyanide to determine the composition of carbonate minerals (Dickson, 1966). Point counts (typically 400 points per thin section) were conducted on selected samples for modal analysis and to determine the nature and volume of rock constituents.

Scanning electron microscopy (SEM), carbon and oxygen isotopic analyses, and fluid inclusion analyses were performed on selected samples. The SEM, equipped with an energy dispersive analyzer of X-rays (EDAX), was used to refine details of paragenetic relations and mineral composition in gold-coated samples. Polished thin sections were also coated with gold and used in the SEM to determine the composition and distribution of elements of some authigenic phases. Semi-quantitative analyses were performed using the combined SEM-EDAX system to obtain approximate elemental composition of authigenic carbonates.

Carbon and oxygen isotope compositions were determined on 18 samples containing authigenic carbonates. The samples selected contained a single or dominant authigenic carbonate species, identified through careful petrographic and X-ray diffraction analyses. Isotopic measurements were made on CO_2 that was produced by reaction of phosphoric acid on calcite-bearing samples for six hours at 25°C. Samples containing siderite were heated to 150°C to obtain CO_2 for isotopic analysis. The oxygen isotope fractionation factor between the acid-extracted CO_2 and siderite at 150°C is 1.00771 (Rosenbaum and Sheppard, 1986). In this paper, we report isotopic data as $\delta^{13}C$ and $\delta^{18}O$, which represent the permil difference in the ratio of $^{13}C/^{12}C$ or $^{18}O/^{16}O$ in the sample to that of the PDB standard (*Belemnitella americana* from the Cretaceous Peedee Formation in South Carolina). The reported oxygen isotope values can be converted to values relative to standard mean ocean water (SMOW) using the relationship $\delta_{SMOW} = (\delta_{PDB} + 29.94)/0.97006$.

The nature of the gases (organic and inorganic) contained in fluid inclusions was assessed by the new technique of fluid inclusion stratigraphy (FIS). This technique was used because most of the samples contain authigenic carbonate phases that were either too small (<10 μm) or the inclusions were too small to

Table 1 - Modal analyses (in percent) for selected sandstone samples, Milk River Formation. Qtz, quartz; Dol; dolomite; Feld, feldspar, dominantly potassium feldspar; RF, rock fragments, dominantly sedimentary including chert, shale, and mudstone; Glauc, glauconitic grains; Corg, organic detritus; IGV, intergranular volume (sum of all cements and primary porosity). Clay percentages include both smectite and kaolinite. Core #, see Figure 1 for core location. Sample number includes well identification/location followed by sample depth (*, depth in metres; **, depth in feet).

		Percent Detrital Grains						Percent Cements and Porosity						
Sample Number	Core #	Qtz	Dol	Feld	RF	Glauc	Corg	Siderite	Calcite	Clay	Pyrite	Primary Porosity	Secondary Porosity	Percent IGV
4-25-14-28W3 423*	10	52.5	4.3	0	14.0	2.5	1.0	6.5	13.8	1.8	2.0	0	1.8	24.1
4-25-14-28W3 425.4*	10	54.8	5.5	0.3	11.8	1.8	1.0	2.8	15.5	3.3	3.5	0	0	25.1
6-22-17-28W3 457.7*	9	39.8	14.0	0.5	13.5	0.5	0.5	1.5	27.5	1.3	0.8	0.3	0	31.4
6-22-17-28W3 444.13*	9	43.3	2.8	0.8	23.8	1.0	4.3	0	0.3	2.8	3.0	18.0	0.3	24.1
6-22-17-28W3 460.25*	9	56.0	7.8	0	12.8	0.8	2.0	1.3	15.5	2.3	1.3	0	0.5	10.4
4-3-15-3W4 1288**	5	42.0	4.3	2.3	25.3	0.8	5.8	0.8	0	2.5	1.0	14.0	1.5	18.3
4-25-14-28W3 1403**	10	42.0	2.8	2.0	28.0	0.3	3.3	0	0	2.8	2.3	15.3	1.5	20.4
3-24-15-28W3 442*	11	37.3	4.7	2.3	26.0	1.0	4.3	0.7	2.7	3.0	0	16.0	2.0	22.4
10-12-10-29W3 562.3*	6	40.3	6.7	2.3	32.0	1.3	4.7	0	0	2.0	2.0	7.3	1.3	11.3
10-12-10-29W3 566.2*	6	45.5	6.3	0.8	26.0	1.5	2.8	0.8	1.3	1.5	1.8	11.0	1.0	16.4
10-23-14-30W3 1567.5**	12	35.7	5.2	1.7	21.7	0	1.7	0	28.7	0.9	1.7	0.9	1.7	32.2

successfully obtain analyses by a more conventional optical-based system using polished thin sections. Also, FIS analysis allows detection of species, both organic and inorganic, that cannot be evaluated with optical-based methods. Nine samples were carefully selected for fluid inclusion studies, based on detailed petrography, isotopic analyses, and X-ray diffraction analyses. In seven samples, siderite was the only or dominant carbonate phase present whereas the other two contained abundant calcite with little or no siderite. The selected samples were first washed to ensure that surfaces were free of volatile contaminants, then placed along with standards, in a vacuum chamber that was pumped (10^{-5} bars) to reduce water and hydrocarbon contents to acceptable levels. Bulk fluid-inclusion volatiles were liberated by mechanical crushing of the samples, and were pumped through four quadrupole mass spectrometers for ionization and separation according to their mass-to-charge ratio. Petroleum species with as many as 13 carbon atoms, as well as inorganic gases, were measured, and compounds with an abundance range of six orders of magnitude were detected and processed.

The volatiles analyzed by the FIS technique represent a composite of all inclusions in the sample and are not from individual inclusions as would be the case using an optical-based system. This technique provides important information because the samples were carefully selected to ensure that they were dominated by the authigenic phase of interest. Hence, indications of hydrocarbons and/or bacterially derived volatile compounds suggest that the processes that formed them occurred during or after precipitation of the host mineral phase. At least three replicates of each sample were run for quality control and to determine the variability of the volatile content of fluid inclusions.

4. Post-depositional Alteration History

Post-depositional alterations in the Milk River Formation include dissolution of detrital constituents, precipitation of authigenic minerals, and compaction. The nature and relative timing of these events are summarized in Figure 6, which is a compilation of data from core, including sandstone, siltstone, and mudstone, from across the study area. Although all the events shown were not generally found in any individual sample, several were consistently present in many samples and were used to establish an overall paragenetic sequence of alterations for the formation.

a) Authigenic Minerals

Milk River authigenic cements include silicates, sulphides, and carbonates (Figure 6). Most cement types that formed throughout the alteration history of the unit occur in relatively minor amounts and do not appear to have any relation to methanogenesis. Thus, these cements, principally the silicates and sulphides, will be only briefly discussed. Emphasis has instead been placed on authigenic carbonate minerals because

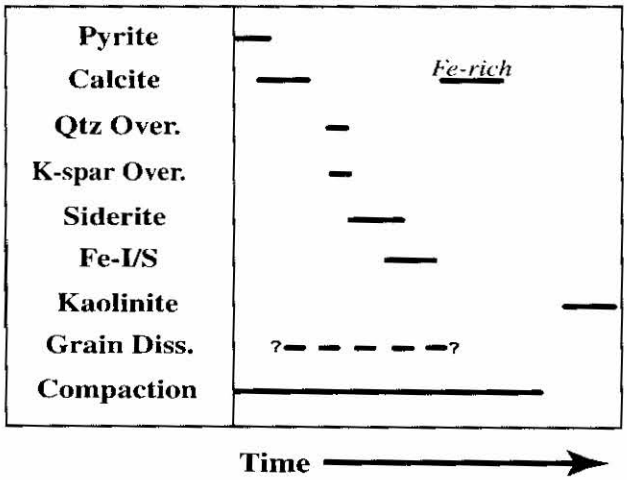

Figure 6 - Diagram showing nature and relative timing of alterations in the Milk River Formation. Diagenetic events represent precipitation of minerals unless otherwise noted. (Qtz, quartz; Over., overgrowth; K-spar, potassium feldspar; Fe-I/S, iron-rich smectite; Fe, iron; and Diss., dissolution).

they are either volumetrically significant or can be linked to methanogenesis.

Silicates

Authigenic silicate cements in sandstones and siltstones include small quartz and potassium feldspar overgrowths, iron-rich smectite, and kaolinite. SEM observations reveal that the overgrowths are typically <10 μm across, and modal analyses indicate that they comprise less than 1% of the rock volume. Iron-rich smectite appears to have developed relatively early (Figure 6), whereas kaolinite was the last to form. Smectite coats detrital grain surfaces or previously formed authigenic minerals. This relationship helps to establish the position of smectite in the paragenetic sequence (Figure 6). Kaolinite is present as relatively large (>20 μm in length) worm-like masses and occurs on all earlier authigenic minerals. Both clay types are best developed in sandstone, although they are also present in other lithologies.

Pyrite

Pyrite occurs as framboids ≤20 μm across and as masses (>50 μm across) of pyrite crystallites (each crystallite ≤2 μm across). Pyrite is ubiquitous but volumetrically most significant in mudstone and siltstone. In sandstones, pyrite typically comprises <4% of the rock volume (Table 1), although locally as much as 11%. Pyrite was observed to be cemented by later siderite and calcite (Figure 6), which is the same sequence of authigenesis observed in rocks of similar age and depositional setting in the Western Interior of the United States (Gautier, 1982) and in marine sediments in general (Nissenbaum *et al.*, 1972; Claypool *et al.*, 1973; Claypool and Kaplan, 1974; Irwin *et al.*, 1977).

Siderite

Authigenic siderite was observed in all lithologies in the Milk River Formation and formed relatively early (Figure 6). It is present in interstices in sandstone and siltstone as rhombic crystals <10 μm across (Figure 7A) and as overgrowths (up to 50 μm) on detrital dolomite grains (Figure 7B). Both forms of siderite typically occupy only 7% or less of the rock volume (Table 1). The siderite in these clastic rocks contains (by weight) as much as 16% MgO and/or as much as 16% CaO with the remainder being FeO. This amount of impurity is diagnostic of authigenic siderite that forms from marine waters in which Mg^{2+} and Ca^{2+} are abundant. In contrast, siderite that forms from meteoric water in continental environments is typically pure $FeCO_3$ (Mozley, 1989; Mozley and Carothers, 1992).

Siderite also occurs in large (maximum height about 15 cm, with horizontal dimensions limited by the diameter of core) concretionary masses that typically formed at lithofacies boundaries (Figure 5). In addition to the mosaic of interlocking 5 to 7 μm-diameter rhombic siderite microcrystals (Figure 7C), the concretions contain clay and minor amounts of authigenic pyrite and quartz or detritus of quartz, pelloids, glauconitic grains, organic material, and fossil fragments. Concretionary siderite is compositionally similar to siderite cement and overgrowths, indicating that all authigenic siderite studied in the Milk River Formation formed contemporaneously and from waters of similar chemical composition. That the siderite formed early in the post-depositional history of the formation is also indicated by the condition of ductile grains in concretions; little or no deformation was observed for grains such as glauconite, delicate pelloids, organic detritus, or rare fossil fragments. Deformation of these delicate grains would likely have begun during shallow burial if little or no siderite had formed early to create a competent preservative framework.

Carbon isotopic values ($\delta^{13}C$) for authigenic siderite in concretions range from -1.99 to -14.23 ‰ and oxygen ($\delta^{18}O$) from -10.87 to -19.41 ‰ (Figure 8). These ranges are consistent with an origin from marine waters (Mozley and Wersin, 1992). The $\delta^{13}C$ values also fall in the range with those of siderite formed during methanogenesis (Claypool and Kaplan, 1974; Gautier,

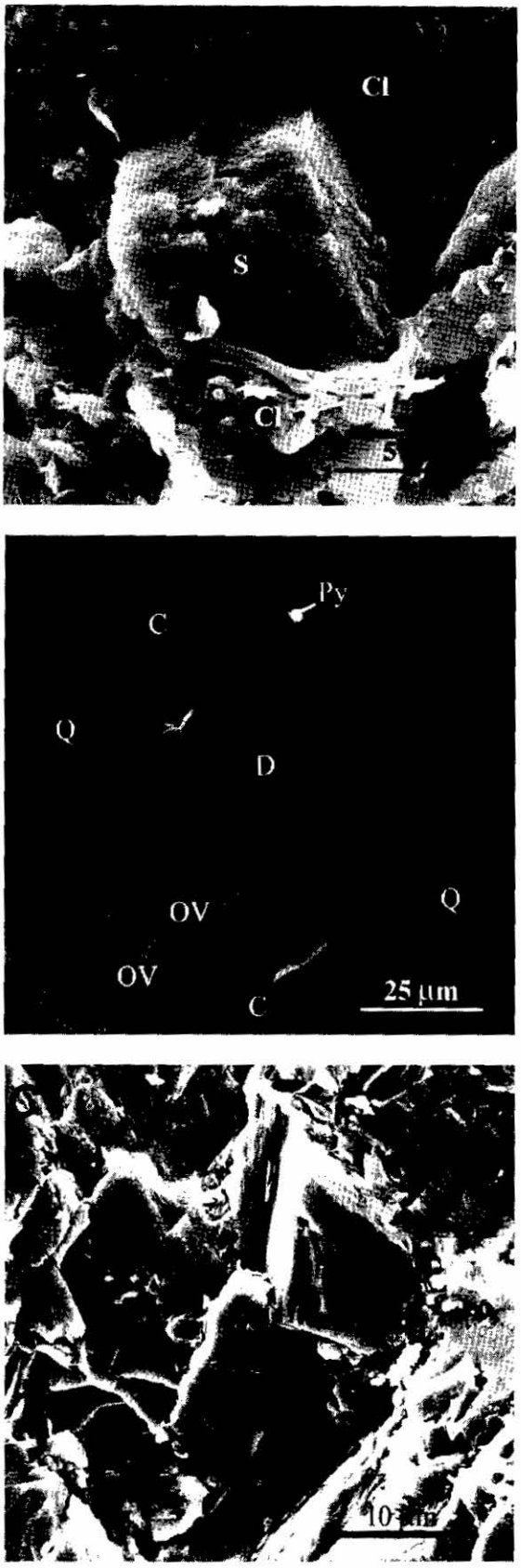

Figure 7 - Scanning electron photographs of siderite in the Milk River Formation. See Figure 1 for all sample locations.
A) Early siderite (S) overlain by or possibly intergrown with iron-rich smectite clay (Cl). Sample (number 6-22-17-28W3, 455.4 m) is from core 9.
B) Back-scattered electron image of siderite overgrowth (OV) on detrital dolomite (D). Euhedral shape of detrital quartz (Q) results from the presence of small quartz overgrowths. Later calcite (C) cements both siderite and quartz overgrowths. Pyrite (Py) is enclosed by siderite overgrowth at top of photograph. Sample (number 6-22-17-28W3, 457.7 m) is from core 9.
C) Mosaic of siderite crystallites in a concretionary mass. Sample (number 11-8T-18-29W3, 1541 ft) is from core 8.

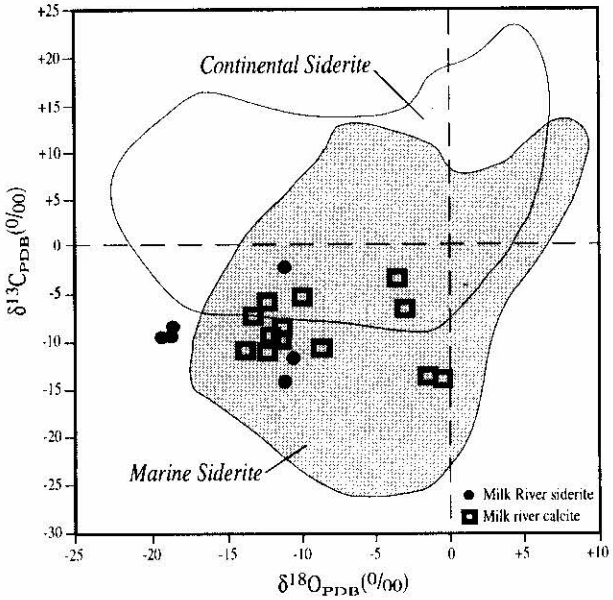

Figure 8 - Plot of $\delta^{13}C$ and $\delta^{18}O$ values for siderite and calcite in the Milk River Formation. Fields for marine and continental siderites taken from Mozley and Wersin (1992). Note that many Milk River Formation samples fall within the field for marine siderite. (Siderite samples are largely from concretions or concretionary masses in mudstone, whereas calcite samples are from sandstone).

1981, 1985). The variable oxygen isotopic values (Figure 8) may be the result of precipitation from waters that were compositionally modified by ongoing water/rock interactions as has been suggested for similar findings elsewhere (Mozley and Wersin, 1992). The fact that several alteration events preceded siderite formation (Figure 6) indicates the occurrence of earlier water/rock interactions which possibly served to shift the oxygen isotopic value of the pore fluids in the Milk River Formation from which the siderite was precipitated. Alternatively, ^{18}O-enriched seawaters may have resided, at least periodically, in the Western Interior Seaway as a result of higher than normal input of freshwater into the Cretaceous sea (Tourtelot and Rye, 1969; Kaufmann and Scholle, 1977; Pratt, 1985; Arthur *et al.*, 1985; Pratt *et al.*, 1993; Pagani and Arthur, 1998). If so, pore waters in the Upper Cretaceous marine sediments may also have been enriched in ^{18}O. The possibility that an almost 9 ‰ variability in $\delta^{18}O$ values was caused by the effects of temperature is unlikely because the Milk River Formation was not buried deeply enough. Moreover, all the siderite in the Milk River Formation occurs in the same paragenetic position, which indicates that all formed at approximately the same time and thus probably under similar temperature conditions.

Fluid inclusion studies indicate that siderite formed during methanogenesis. All seven sideritic concretionary samples analyzed for fluid inclusions contained methane (Figure 9) as well as other volatile compounds usually associated with bacterial processes (for example, acetic acid ±COS, CS_2, and H_2S). Given that the samples were evacuated prior to analysis to remove any possible traces of hydrocarbons that might have been in the pores, the analyses point to inclusions in the siderite as the source of methane and other bacterially mediated compounds. We believe that the fluid inclusions in the siderite are primary for the following two reasons: (1) siderite is stable and does not typically recrystallize during diagenesis (Curtis *et al.*, 1975; Gould and Smith, 1979; Matsumoto and

Core Number	*Sample Number*	*Minerals Present*	*Methane*
14	4-18-14-27W3 1866*	*siderite, quartz*	
10	4-25-14-28W3 425.4	*calcite, quartz*	
9	6-22-17-28W3 420.6	*siderite, quartz*	
9	6-22-17-28W3 460.2A	*siderite, quartz trace calcite*	
9	6-22-17-28W3 460.2B	*calcite, quartz*	
9	6-22-17-28W3 467.6	*siderite, quartz*	
8	11-8T-1829W3 1541*	*siderite*	
13	15-32-14-10 1468.7*	*siderite*	
14	16-34-13-28W3 1351*	*siderite, quartz*	

1 5 10

Millivolts (x 10^5)

Figure 9 - Fluid inclusion–mass spectrometric analyses for methane in samples from the Milk River Formation. Also shown are the core and sample numbers (*, depth in feet; other depths are in metres), and the minerals present as indicated by X-ray diffraction analysis.

Iijima, 1981; Gautier, 1982; Curtis and Coleman, 1986); and (2) analytical or other evidence of post-siderite alteration such as compositional variations or fractures are lacking within the samples studied. Although trace amounts of higher hydrocarbons ($>C_1$) were also detected from the fluid-inclusion analyses, their presence is not surprising because they are known to occur even in biogenic gas systems in recent sediments (Weber and Maximov, 1976; Claypool and Kvenvolden, 1983).

Calcite

Authigenic calcite formed both before and after precipitation of siderite (Figure 6); however, the composition of these two generations of calcite differs.

Early-formed calcite is highly calcic, as indicated from the staining of thin sections. This calcite occurs as an interstitial cement in sand-filled burrows, but such occurrences are areally and volumetrically insignificant compared to the amount of calcite precipitated after siderite in the Milk River Formation (see Figure 7B).

The later generation of calcite is a poikilotopic cement in sandstone and siltstone in volumes ranging from <1% to as much as 28.7% (Table 1). It is variable in composition, as determined from stained thin sections. Overall, the iron content decreases toward the centre of interstitial pores indicating that pore waters responsible for calcite formation evolved from a more iron-rich to iron-depleted state. The $\delta^{13}C$ composition of the calcite ranges from -3.68 to -14.02 ‰ and the $\delta^{18}O$ composition from -0.63 to -13.16 ‰ (Figure 8). Because these isotopic values represent bulk sample analysis, it is unclear whether the variability in $\delta^{13}C$ and $\delta^{18}O$ corresponds to changes in the iron content of the calcite. Nevertheless, significant overlap of calcite and siderite isotopic values is evident (Figure 8). As such, the isotopic signature of the calcite is consistent with its formation from marine waters. In addition, the $\delta^{13}C$ values also fall within the range of values expected for minerals that formed during methanogenesis (Claypool and Kaplan, 1974; Gautier, 1981; Claypool and Kvenvolden, 1983; Gautier, 1985). As with siderite, the variability of $\delta^{18}O$ values for the calcite indicates that it may have formed from marine waters that had evolved isotopically due to water/rock interactions or from ^{18}O-enriched marine waters, or from a combination of both.

Fluid inclusion studies also suggest that the calcite formed during methanogenesis. Although only two samples containing abundant calcite cement were analyzed, both contained methane in submicroscopic fluid inclusions (Figure 9) as well as other volatile compounds usually associated with bacterial processes (for example acetic acid ± COS, CS_2, and H_2S). The interpretation that methane and other bacterially generated compounds liberated during fluid inclusion analysis is in the authigenic calcite and not the detrital quartz is supported by petrographic observations, which indicate that the quartz grains were derived largely from igneous and metamorphic source rocks. Although methane can occur in fluid inclusions in quartz from metamorphic or igneous rocks, the presence of bacterially mediated compounds cannot. As with siderite, trace amounts of other hydrocarbons were also detected during fluid inclusion analyses of the calcite; this can be expected for carbonates that form in biogenic gas systems (Weber and Maximov, 1976).

b) Compaction

Sandstone beds in the Milk River Formation display textural features that indicate they have undergone varying degrees of compaction. Intergranular volumes (IGV; volume of the rock that is primary pore space plus authigenic cement; see Houseknecht, 1987) in sandstone beds range from 11.3 to 32.2% (Table 1), whereas the original porosity of these sandstone beds is postulated to have been about 35% (original porosity estimated from information in Beard and Weyl (1973) and Carozzi, (1993)). Based on the relation between the observed IGV and the estimated original porosity, a sandstone bed with an IGV of 32% has experienced about a 9% reduction in porosity ((35% to 32%)/35% = 9%), whereas an IGV of 11.3% indicates a 65% reduction in porosity. The IGV of sandstone beds completely cemented with calcite ranges from about 20 to 32% (Table 1). This range suggests that calcite cementation began when the IGV of sandstone beds was about 32% and continued until the IGV had dropped to about 20% (a 43% reduction in porosity) due to burial compaction. Sandstone beds lacking calcite cement have IGV values ranging from about 11 to 24% (Table 1). These generally lower values imply that compaction was greater in these beds than in calcite-cemented beds, which in turn suggests that calcite cementation ended before burial compaction had concluded in the Milk River Formation. Compaction was most significant in beds containing little or no calcite.

Textural features corroborate the timing of calcite cementation relative to maximum burial. Petrographic observations show that sandstone beds lacking calcite cement display more ductile grain (sedimentary rock fragments and glauconitic grains) deformation than sandstone beds with abundant calcite. Moreover, sandstone beds with little or no calcite cement and abundant ductile grains have experienced the greatest volume of porosity loss due to compaction (up to 65%). Thus calcite cementation must have ended prior to maximum burial of the Milk River Formation.

5. Timing of Gas Generation

The detailed petrologic studies of the Milk River Formation have been useful in establishing the nature and timing of authigenic siderite and calcite formation and in linking the timing of methane generation to that of siderite and calcite precipitation. Several lines of reasoning point to early formation of siderite in both a relative and absolute sense in the post-depositional history of the Milk River Formation. First, the elemental and isotopic composition of siderite is

indicative of a carbonate that formed from marine waters. Thus, siderite precipitation had to occur when sufficient marine waters were still present in the sediments, which is likely to be shortly after deposition but before extensive dewatering from compaction. Secondly, siderite is present as large overgrowths on detrital dolomite in sandstone and siltstone (Figure 7B); large overgrowths require large empty pore spaces in which to grow and such large pores would not have survived much cementation and compaction. Thirdly, ductile and fragile grains in concretions show little or no evidence of deformation, indicating that they were encased within a rigid authigenic siderite framework early in the post-depositional history of the rock, which allowed for preservation of their delicate textures and shapes. Deformation of ductile grains would have begun after minimal lithostatic pressure due to shallow burial, and would have become more intense with increasing burial depth.

The link between siderite formation and methanogenesis, indicated by the presence of methane-bearing inclusions within the siderite, helps to corroborate an early timing for methanogenesis in the Milk River Formation. Although the carbon isotopic composition of siderite is indicative of a methanogenic source for carbon, the presence of methane in presumed primary fluid inclusions provides a temporal link between methanogenesis and siderite formation. The presence of methane during siderite formation is consistent with observations from ocean-drilling projects that have found authigenic siderite in the zone of methanogenesis (Claypool and Kaplan, 1974; Rodriguez *et al.*, 2000).

A temporal link between methanogenesis and post-sideritic alterations is further supported by petrologic data. The presence of methane in fluid inclusions in the later generation of calcite cement implies that methanogenesis continued at least through the time of calcite precipitation. Thus, methane generation appears to have spanned a significant amount of time during the post-depositional alteration of the Milk River Formation.

The minimum duration of methane generation can be broadly bracketed by combining petrographic observations from the sample suite used in this study with results of studies on marine sediments obtained through ocean-drilling projects. Methane generation probably began in the Milk River Formation shortly after deposition (t_1 on Figure 10), after sulphate in the pore waters was largely consumed in the formation of early pyrite (see Figure 6). Methane generation can only occur after virtually all sulphate is removed from the pore waters because small amounts of sulphate can inhibit the growth of methanogens, the bacteria responsible for methane generation (Claypool and Kaplan, 1974; Gautier, 1985). Depletion of sulphate and the associated ending of pyrite precipitation then allows for an increase in the Fe^{2+} activity, which favours precipitation of siderite. Siderite formation also probably began slightly after the start of methane generation.

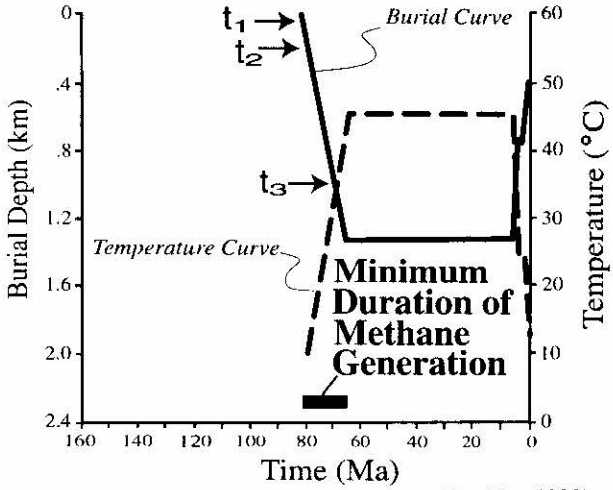

Figure 10 - Burial curve (from Corbet and Bethke, 1992) for the Milk River Formation along an east-west line in southern Alberta, at a latitude that approximately parallels Township 1 N, with times t_1, t_2, and t_3 (see text for explanation of the significance of t_1, t_2, and t_3). The minimum duration of principal gas generation, times t_1 to t_3, was determined in the present study to approximately bracket the timing of methanogenesis in the Milk River Formation.

After the end of siderite precipitation, probably owing to depletion of available iron from pore fluids, methanogenesis continued as indicated by methanic inclusions in the later calcite. The later calcite cementation, however, did not commence until there was at least a 9% reduction in porosity of Milk River Formation sandstone beds due to burial compaction (see earlier discussion). A reduction in porosity of about 9% is estimated (estimations, made following results of experimental studies of compaction by Pittman and Larese (1991), are based on grain size, sorting, and volume of ductile grains) to have occurred after the Milk River Formation was buried to about 200 m (t_2, Figure 10). Calcite in sandstone beds continued to form contemporaneously with methane generation until a porosity reduction of up to 43% was reached (see Table 1).

The fact that sandstone beds lacking calcite cement compacted more than 43% indicates that calcite cementation ceased prior to maximum burial. Although primary methanogenesis is not observed today in marine sediments below burial depths of about 1 kilometre (Rice and Claypool, 1981), microbial communities have been discovered in more deeply buried rocks (Scott *et al.*, 1994; Martini *et al.*, 1998), allowing for speculation that biogenic gas can be generated at greater depths.

These observations broadly indicate that methanogenesis continued at least until the Milk River Formation had been buried to about one kilometre (t_3, Figure 10) and possibly to the maximum burial depth of 1.3 kilometres. Methane generation in the Milk River Formation appears to have spanned at least 15 m.y. from time of sediment deposition until about 65 Ma. If methanogenesis continued after the strata

were buried only slightly deeper than one kilometre, its duration would lengthen significantly (see Figure 10). Although methanogenesis occurred early in the post-depositional history of the formation, the gas appears to have remained in the formation, perhaps in pore fluids, because of very low permeability, which is in part a function of methane-related diagenesis. The gas probably remained in solution until rapid uplift in the region, which began about 7 to 8 Ma (see Figure 3), when a significant reduction in hydrostatic and lithostatic pressures resulted in its exsolution. Nevertheless, the isotopic composition of the exsolved gas in the Milk River Formation, along with the constraints placed on the timing of generation, indicate that the gas is primary and biogenic, not a younger generation of biogenic gas that was generated after uplift and flushing with fresh water as proposed by Martini *et al.* (1998) for biogenic gas in the Antrim Shale in the Michigan Basin.

6. Conclusions

Based on petrologic, isotopic, and fluid inclusion studies of the Cretaceous Milk River Formation in southeastern Alberta and southwestern Saskatchewan, the timing of biogenic methane generation can be estimated and the duration of methanogenesis broadly bracketed. Siderite, an authigenic cement, was precipitated during methanogenesis as indicated by the presence of methanic fluid inclusions. The carbon and oxygen isotopic signature of siderite is a further indication that it formed during methane generation. Authigenic calcite cementation followed precipitation of siderite, but isotopic similarities between the two minerals indicate that they formed from pore fluids of similar isotopic composition. The presence of methane in fluid inclusions in the calcite provides additional evidence that methanogenesis spanned the interval of both siderite and calcite formation. A consideration of: 1) the textural features of Milk River sandstone beds, 2) their burial history, and 3) the observed relations of methanogenesis in modern marine sediments, indicates that methane generation started soon after deposition of the Milk River Formation and continued for at least 15 m.y. and perhaps longer. Further work will include: 1) additional analyses on the authigenic carbonate minerals, and 2) dating of the waters co-produced with methane to determine their age and whether or not they are in equilibrium with the methane. Results from these future efforts will further constrain models for gas accumulation and trapping in the Milk River Formation.

7. Acknowledgments

This manuscript was greatly improved by the technical reviews of George Claypool and Mitch Henry and editorial review of Richard Keefer. We are also appreciative of the many helpful conversations we had about this work with George Claypool, Don Gautier, and Marty Parris. Clay-mineral analyses were kindly performed by Dennis Eberl, and we thank him for his assistance. This work was funded by the Energy Resources Program of the U.S. Geological Survey.

8. References

Arthur, M.A., Dean, W.E., Pollastro, R.M., Scholle, P.A., and Claypool, G.E. (1985): A comparative geochemical study of two transgressive pelagic limestone units, Cretaceous western interior basin, U.S.; *in* Pratt, L.M., Kauffman, E.G., and Zelt, F.B. (eds.), Fine-grained deposits and biofacies of the Cretaceous Western Interior Seaway–evidence of cyclic sedimentary processes; Soc. Econ. Paleont. Mineral., 1985 Midyear Mtg., Field Trip Guidebook 4, p16-27.

Attanazi, E.D. and Schmoker, J.W. (1997): Long-term implications of new U.S. gas estimates; Nonrenew. Resour., v6, p53-62.

Beard, D. and Weyl, P. (1973): Influence of texture on porosity and permeability of unconsolidated sand; Amer. Assoc. Petrol. Geol. Bull., v57, p349-369.

Bernard, B.B., Brooks, J.M., and Sackett, W.M. (1976): Natural gas seepage in the Gulf of Mexico; Earth Planet. Sci. Lett., v31, p45-54.

Carozzi, A.V. (1993): Sedimentary Petrography; Prentice Hall, Englewood Cliffs, 263p.

Claypool, G.E. and Kaplan, I.R. (1974): The origin and distribution of methane in marine sediments; *in* Kaplan, I.R. (ed.), Natural Gases in Marine Sediments; Plenum Press, New York, p99-139.

Claypool, G.E. and Kvenvolden, K.A. (1983): Methane and other hydrocarbon gases in marine sediment; Ann. Rev. Earth Planet. Sci., v11, p299-327.

Claypool, G.E., Presley, B.J., and Kaplan, I.R. (1973): Gas analyses in sediment samples from Legs 10, 11, 13, 14, 15, 18, and 19; Initial Report, Deep Sea Drilling Project, v19, p879-884.

Corbet, T.F. and Bethke, C.M. (1992): Disequilibrium fluid pressures and groundwater flow in the western Canada sedimentary basin; J. Geophys. Resear., v97, noB5, p7203-7217.

Creaney, S., Allen, J., Cole, K.S., Fowler, M.G., Brooks, P.W., Osadetz, K.G., Macqueen, R.W., Snowden, L.R., and Riediger, C.L. (1994): Petroleum generation and migration in the Western Canada Sedimentary Basin; *in* Mossop, G.D. and Shetsen, I., (comp.), Geological Atlas of the Western Canada Sedimentary Basin; Can. Soc. Petrol. Geol./Alta. Resear. Counc., p455-468.

Curtis, C.D. and Coleman, M.L. (1986): Controls on the precipitation of early diagenetic calcite, dolomite, and siderite concretions in complex depositional sequences; *in* Gautier, D.L. (ed.), Roles of organic matter in sediment diagenesis,

Soc. Econ. Paleont. Mineral., Spec. Publ. 38, p23-33.

Curtis, C.D., Pearson, M.J., and Somogyi, V.A. (1975): Mineralogy, chemistry, and origin of a concretionary siderite sheet (clay-ironstone band) in the Westphalian of Yorkshire; Mineral. Mag., v40, p385-393.

Dickson, J.A.D. (1966): Carbonate identification and genesis as revealed by staining; J. Sed. Petrol., v36, p491-505.

Energy Resources Conservation Board (1977): Alberta's reserves of crude oil, gas, natural gas liquids, and sulphur at 31 December 1977; Energy Resour. Conserv. Board, Rep. 78-18, 308p.

Fuex, A.N. (1977): The use of stable carbon isotopes in hydrocarbon exploration; J. Geochem. Expl., v7, p155-188.

Gautier, D.L. (1981): Relationship of organic matter and mineral diagenesis–report of the 1983 Society of Economic Paleontologists and Mineralogists Research Conference; J. Sed. Petrol., v54, p1028-1032.

_____ (1982): Siderite concretions–indicators of early diagenesis in the Gammon Shale (Cretaceous); J. Sed. Petrol., v52, p859-871.

_____ (1985): Interpretation of early diagenesis in ancient marine sediments; Relationship of Organic Matter and Mineral Diagenesis, Soc. Econ. Paleont. Mineral., Short Course 17, p6-72.

Gould, K.W. and Smith, J.W. (1979): The genesis and isotopic composition of carbonates associated with some Permian Australian coals; Chem. Geol., v24, p137-150.

Hankel, R.C., Davies, G.R., and Krouse, H.R. (1989): Eastern Medicine Hat gas field–a shallow, Upper Cretaceous, bacteriogenic gas reservoir of southeastern Alberta; Bull. Can. Petrol. Geol., v37, p98-112.

Houseknecht, D.W. (1987): Assessing the relative importance of compaction processes and cementation to reduction of porosity in sandstones; Amer. Assoc. Petrol. Geol. Bull., v71, p633-642.

Irwin, H., Curtis, C.D., and Coleman, M. (1977): Isotopic evidence for source of diagenetic carbonates formed during burial of organic-rich sediments; Nature, v269, p209-213.

Kauffman, E.G. and Scholle, P.A. (1977): Abrupt biotic and environmental changes during peak Cretaceous transgressions in Euramerican; *in* North American Paleontology Convention II, Abstracts, J. Paleont., v51, p16.

Martini, A.M., Water, L.M., Budai, J.M., Ku, T.C.W., Kaiser, C.J., and Schoell, M. (1998): Genetic and temporal relations between formation waters and biogenic methane–Upper Devonian Antrim Shale, Michigan Basin, USA; Geochim. Cosmochim. Acta, v62, p1699-1720.

Matsumoto, R. and Iijima, A. (1981): Origin and diagenetic evolution of Ca-Mg-Fe carbonates in some coalfields of Japan; Sediment., v28, p239-259.

Mozley, P.S. (1989): Relation between depositional environment and the elemental composition of early diagenetic siderite; Geol., v17, p704-706.

Mozley, P.S. and Carothers, W.W. (1992): Elemental and isotopic composition of siderite in the Kuparuk Formation, Alaska–effect of microbial activity and water/sediment interaction of early pore-water chemistry; J. Sed. Petrol., v62, p681-692.

Mozley, P.S. and Wersin, P. (1992): Isotopic composition of siderite as an indicator of depositional environment; Geol., v20, p817-820.

Nissenbaum, A., Presley, B.J., and Kaplan, I.R. (1972): Early diagenesis in a reducing fjord, Saanich Inlet, British Columbia–I, Chemical and isotopic changes in major components of interstitial water; Geochim. Cosmochim. Acta, v36, p1007-1027.

O'Connell, S., Campbell, R., and Bhattacharya, J. (1999): The stratigraphy, sedimentology, and reservoir geology of the giant Milk River gas field in southeastern Alberta and Saskatchewan; Can. Soc. Petrol. Geol., Ann. Meeting, Abst., p99-83-O.

Pagani, M. and Arthur, M.A. (1998): Stable isotopic studies of Cenomanian-Turonian proximal marine fauna from the U.S. Western Interior Seaway; *in* Dean, W.E. and Arthur, MA. (eds.), Stratigraphy and paleoenvironments of the Cretaceous Western Interior Seaway, USA, Soc. Econ. Paleont. Mineral. Conc. Sediment. Paleont. v6, p201-225.

Pittman, E.D. and Larese, R.E. (1991): Compaction of lithic sands–experimental results and applications; Amer. Assoc. Petrol. Geol. Bull., v75, p1279-1299.

Pratt, L.M. (1985): Isotopic studies of organic matter and carbonate in rocks of the Greenhorn marine cycle; *in* Pratt, L.M., Kauffman, E.G., and Zelt, F.B. (eds.), Fine-grained deposits and biofacies of the Cretaceous Western Interior Seaway–evidence of cyclic sedimentary processes; Soc. Econ. Paleont. Mineral., Midyear Meeting, Field Trip Guidebook 4, p38-48.

Pratt, L.M., Arthur, M.A., Dean, W.E., and Scholle, P.A. (1993): Paleo-oceanographic cycles and events during the Late Cretaceous in the Western Interior Seaway of North America; *in* Caldwell,

W.G.E. and Kauffman, E.G. (eds.), Evolution of the Western Interior Basin, Geol. Assoc. Can., Spec. Pap. 39, p333-353.

Rice, D.D. and Claypool, G.E. (1981): Generation, accumulation, and resource potential of biogenic gas; Amer. Assoc. Petrol. Geol. Bull., v65, p5-25.

Ridgley, J.L. (2000): Lithofacies architecture of the Milk River Formation (Alderson Member of the Lea Park Formation), southwestern Saskatchewan and southeastern Alberta–its relation to gas accumulation; *in* Summary of Investigations 2000, Volume 1, Saskatchewan Geological Survey, Sask. Energy Mines, Misc. Rep. 2000-4.1, p106-120.

Ridgley, J.L., Hester, T.C., Condon, S.M., Anna, L.O., Rowan, E.L., Cook, T., and Lillis, P.G. (1999): Reevaluation of the shallow biogenic gas accumulation, northern Great Plains, USA–is the similar gas accumulation in southeastern Alberta and southwestern Saskatchewan a good analog?; *in* Summary of Investigations 1999, Volume 1, Saskatchewan Geological Survey, Sask. Energy Mines, Misc. Rep. 99-4.1, p64-78.

Rodriguez, N.M., Paull, C.K., and Borowski, W.S. (2000): Zonation of authigenic carbonates within gas hydrate-bearing sedimentary sections on the Blake Ridge–offshore southeastern North America; *in* Paull, C.K., Matsumoto, R., Wallace, P.J., and Dillon, W.P. (eds.), Proceedings of ODP Science Results, 164, College Station, Texas (Ocean Drilling Program), p301-312.

Rosenbaum, J. and Sheppard, S.M.F. (1986): An isotopic study of siderites, dolomites and ankerite at high temperature; Geochim. Cosmochim. Acta v50, p147-1150.

Scott, A.R., Kaiser, W.R., and Auers, W.B., Jr. (1994): Thermogenic and secondary biogenic gases, San Juan basin, Colorado and New Mexico–implications for coalbed gas producibility; Amer. Assoc. Petrol. Geol. Bull., v78, p1186-1209.

Tourtelot, H.A. and Rye, R.O. (1969): Distribution of oxygen and carbon isotopes in fossils of Late Cretaceous age, Western Interior region of North American; Amer. Assoc. Petrol. Geol. Bull., v80, p1903-1922.

Weber, V.V. and Maximov, S.P. (1976): Early diagenetic generation of hydrocarbon gases and their variations dependent on initial organic composition; Amer. Assoc. Petrol. Geol. Bull., v60, p287-293.

Whiticar, M.J., Faber, E., and Schoell, M. (1986): Biogenic methane formation in marine and freshwater environments–CO_2 reduction vs. acetate fermentation-isotopic evidence; Geochim. Cosmochim. Acta, v50, p693-709.